Process Effect on the RMS Roughness of HfO_2 Thin Films Grown by MOMBE

Young-Don Ko, Pyung Moon, and Ilgu Yun[a]
Department of Electrical and Electronic Engineering, Yonsei University, 134 Shinchon-dong, Seodaemoon-gu, Seoul 120-749, Korea

Moon-Ho Ham and Jae-Min Myoung
Department of Metallurgical Engineering, Yonsei University, 134 Shinchon-dong, Seodaemoon-gu, Seoul 120-749, Korea

[a]E-mail : iyun@yonsei.ac.kr

(Received January 8 2007, Accepted March 30 2007)

In this paper, the process effect on the RMS roughness of the HfO_2 thin films grown by metal organic molecular beam epitaxy was investigated. The measured RMS roughness is examined to characterize the surface morphology. In order to analyze the factor effects, the significant factors of both the main and the interaction effects were extracted through the effect analysis. In order to compare the regression model with the variable transformation, the effect of each factor and the model efficiency are calculated. The methodology can allow us to analyze the effects between the process parameters related to the process variability.

Keywords : HfO_2, RMS roughness, Process effect, Factorial design, Regression model, Power transformation

1. INTRODUCTION

The progress of the complementary-metal-oxide-semiconductor (CMOS) technology have been rapidly developed, whereas several problems are not solved yet, which are such as the leakage current, the reliability, the device dimension and the oxide thickness shrinkage. In order to overcome these problems, one of the keys is the scaling of the gate dielectric in CMOS semiconductor technology[1]. For the scaling down, materials used in a gate dielectric have been researched by the various thin film deposition techniques and materials[1-3]. New materials are also considered as the replacement of the former materials for gate dielectric like SiO_2. Due to a high dielectric constant, a high reflective index and a thermal stability, the high-*k* materials are considered as major candidates for the gate oxide, such as TiO_2, ZrO_2, HfO_2, and Ta_2O_5. Those materials can potentially affect the performance of the transistors[4,5].

Generally, properties of thin films can be changed by the various process conditions. Here, HfO_2 thin films grown by metal organic molecular beam epitaxy (MOMBE) process are also characterized by the process control parameters such as the substrate temperature, Ar and O_2 flow rate. The characteristics of thin films can be also determined by the various factors such as the surface morphology, the growth conditions and the crystallity. For this reasons, we focused on the RMS roughness of HfO_2 thin films as the characteristic to be determined the degree of the surface status.

Several researchers have investigated the RMS roughness of thin films to be mainly considered as one of the properties of characteristic[6,7]. For analyzing the response for the semiconductor process, the design of experiments (DOE) has been widely used to predict a model[8,9]. Factorial design and macromodel using regression analysis had been applied to IC fabrication processes by K. K. Low and Stephen W. Director[10]. Keun Park *et al.* researched injection modeling processes using the DOE considering the interaction effect and observed that improved productivity with a high product quality[11]. In addition, M. Hajeeh investigated which factors in the process cause corrosion damaging to the equipments and materials. As a statistical methodology, factorial design and factor effect analysis are used[12].

In this paper, the factor effects were calculated and the significant factors were then selected as the factors to build a model. Based on those factors, the general regression and Box-Cox transformation regression models had been developed and the effects of the model were observed through the response surface plots.

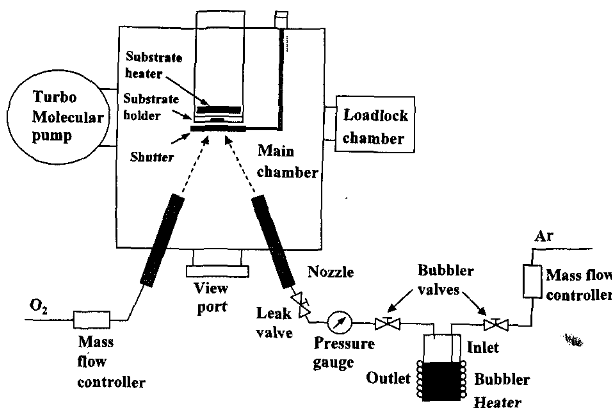

Fig. 1. The schematic of MOMBE systems.

2. EXPERIMENTS

HfO_2 thin film was grown on a p-type Si (100) substrate, of which the native oxide was chemically eliminated by (50:1) H_2O: HF solution prior to the growth by MOMBE. Hf-t-butoxide [Hf $(O{\cdot}t\text{-}C_4H_9)_4$] was chosen as the metal organic (MO) precursor because it has an appropriate vapor pressure and relatively low decomposition temperature. High –purity (99.999 %) oxygen gas was used as the oxidant. Hf-t-butoxide was introduced into the main chamber using Ar as a carrier gas through a bubbling cylinder. The bubbler was maintained at a constant temperature to supply the constant vapor pressure of Hf-source. The apparatus of the system is schematically shown in Fig. 1. High-purity Ar carrier gas passed through the bubbler containing the Hf-source. The gas line from the bubbler to the nozzle was heated to the same temperature. The mixture of Ar and metal-organic gases heated at the tip of the nozzle flows into the main chamber. The introduced Hf-source decomposed into Hf and ligand parts when it reached a substrate maintained at high temperature and Hf ion was combined with O_2 gas supplied from another nozzle. The base pressure and working pressure were $\sim10^{-9}$ and $\sim10^{-7}$ Torr, respectively. The HfO_2 films grown by MOMBE were annealed at 700 °C for 2 minutes in N_2 ambient. The process conditions are summarized in Table 1.

Au dots were deposited to evaluate the electrical properties of grown HfO_2 sample. The stainless shadow mask was used to make regular Au dots and the hole diameter in the mask was 0.2 mm. The determination of the electrode metal and accurate definition of electrode area has influence on the analysis of the electrical properties of HfO_2.

The samples were scanned over the areas of 1×1 um^2 using PSI Auto Probe, and scan rate was 1 Hz. Root mean square (rms) and average roughness were measured by the scanned image of surface.

Table 1. Summary of process conditions.

Process variables	Range
Substrate temperature	450 °C ~ 550 °C
Bubbler temperature	130 °C (Fixed)
Nozzle temperature	270 °C (Fixed)
Base pressure	10^{-9} Torr
Working pressure	10^{-7} Torr
Gas flow (Ar)	3~5 sccm
Gas flow (O_2)	3~5 sccm
Growth time	30 min

Table 2. Factorial design matrix.

Run	T_{sub} [℃]	Ar [sccm]	O_2 [sccm]	RMS roughness [Å/㎛^{2}]	Remark
1	450	3	3	8.796	Full Factorial design
2	450	3	5	10.061	
3	450	5	3	4.906	
4	450	5	5	6.674	
5	550	3	3	2.448	
6	550	3	5	2.463	
7	550	5	3	2.798	
8	550	5	5	2.732	
9	500	4	4	9.984	Center point

3. MODELING SCHEME

3.1 Design of Experiments

In order to characterize the high-*k* dielectric properties, the input factors were extracted with respect to the controllable process variables of MOMBE equipment. Those factors are the substrate temperature (T_{sub}), Ar gas flow (Ar) and O_2 gas flow (O_2). Generally, the factorial design creates two levels of each factor, which are called 'high' and 'low' respectively. The full factorial design specifies factorial design with all possible high (+) / low (-) combination of all the input factors. In order to consider the curvature effect, the design of two-level factors with center points is carried out[12]. The full factorial design matrix with one center point was summarized in Table 2.

3.2 Regression model and power transformation

These regression models have the following form:

$$y=\alpha_0+\alpha_1u_1+\alpha_2u_2+\alpha_3u_3+\alpha_4u_1u_2+\alpha_5u_1u_3+\alpha_6u_2u_3+\varepsilon \quad (1)$$

where y is a response variable, u_i's are the three process variables varied in the full factorial design with a center point, α_i's are regression coefficients estimated using the least squares method, and ε is a modeling error. These model can be defined the following that;

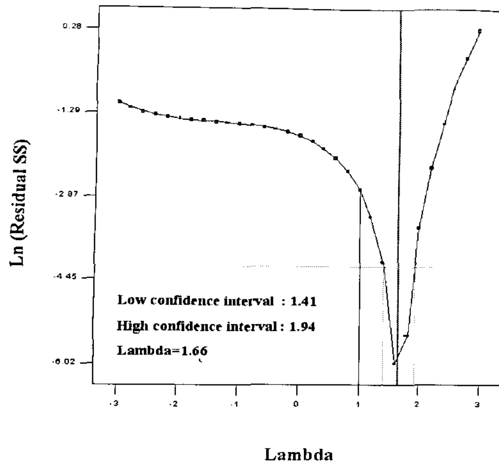

Fig. 2. The Box-cox plot for power transforms.

$$RMS\ roughnes = 55.99919 - 0.098104 \times T_{sub} - 10.70240 \times Ar + 4.22866 \times O_2 + 0.019740 \times T_{sub} \times Ar - 0.007712 \times T_{sub} \times O_2 \quad (2)$$

The variable transformation technique was used to treat the response for a small data set. Generally, there are some purposes for using the variable transformation that are the following[11]; 1) stabilizing response variance, 2) making the distribution of the response variable close to the normal distribution and 3) improving the fit of the model to the data.

Here, one of the power transformations was used in the change of the response. This transformation is $y^* = y^{\lambda}$ that is useful for applying the response variables in the fluctuation process. The transformation parameter can be determined by Box-Cox method[12,13]. The plot of the lambda versus the error sum of squares of lambda is illustrated in Fig. 2 as the Box-cox plot for power transformation. As indicated, the suitable lambda is 1.66, and the low and high confidence interval is from 1.41 to 1.94.

For all suggested models, the higher interaction such as the three factor interaction is not considered in this study as the noise factors. The analysis of variance (ANOVA) is summarized in Table 3-4. From the ANOVA table, excepting the insignificant factors, the main factor, the interaction factor, curvature effect and model were verified through P-values. The adjusted R-squared values for the each model are 0.9965 and 0.9196, respectively. All models were carried out under the significance level is 95 %.

The variable transformation model can be defined the following that;

$$(RMS\ roughness)^{1.66} = 403.78084 - 0.72871 \times T_{sub} - 65.06891 \times Ar + 0.11919 \times T_{sub} \times Ar \quad (3)$$

Table 3. ANOVA table for the regression model.

Source	Sum of Squares	DF	Mean Square	F	P
Model	65.61	5	13.12	404.66	0.0025
$A(T_{sub})$	49.98	1	49.98	1541.16	0.0006
B(Ar)	5.54	1	5.54	170.85	0.0058
$C(O_2)$	1.11	1	1.11	34.30	0.0279
AB	7.79	1	7.79	240.33	0.0041
AC	1.19	1	1.19	36.68	0.0262
Curvature	21.12	1	21.12	651.26	0.0015
Residual	0.065	2	0.032		
Total	86.80	8			

The adjusted R-squared value: 0.9965, DF=Degrees of Freedom
A= T_{sub}, B= Ar and C= O_2.
T_{sub}

Table 4. ANOVA table for the variable transformation model.

Source	Sum of Squares	DF	Mean Square	F	P
Model	1793.60	3	597.87	27.70	0.0039
$A(T_{sub})$	1269.67	1	1269.67	58.82	0.0016
B(Ar)	239.82	1	239.82	11.11	0.0290
AB	284.11	1	284.11	13.16	0.0222
Curvature	700.10	1	700.10	32.43	0.0047
Residual	86.34	4	21.59		
Total	2580.04	8			

The adjusted R-squared value: 0.9196, DF=Degrees of Freedom
A= T_{sub}, B= Ar and C= O_2.

4. RESULTS AND DISCUSSION

AFM images of HfO_2 thin films were illustrated in Fig. 3. AFM images of the test sample having the different process conditions followed by design of experiments were arranged in order. As shown in Fig. 3, it was observed that the surface morphologies for the each sample can not seem to be homogeneous. The various surface morphologies were observed. That could be the more complexity effect on the process circumstance and different conditions.

In order to extract the significant factors in the model, the half normal and normal probability plots for the factors in the regression model were represented in Fig. 4. The large effect factors in the process fluctuation were statistically extracted as the significant factors that are consist of the main and interaction factor. The main factors having the high effect are the substrate temperature, Ar and O_2 flow rate. One of the interaction factors having the high effect is the factor between the substrate temperature and Ar flow rate, the other is the factor between the substrate temperature and O_2 flow rate.

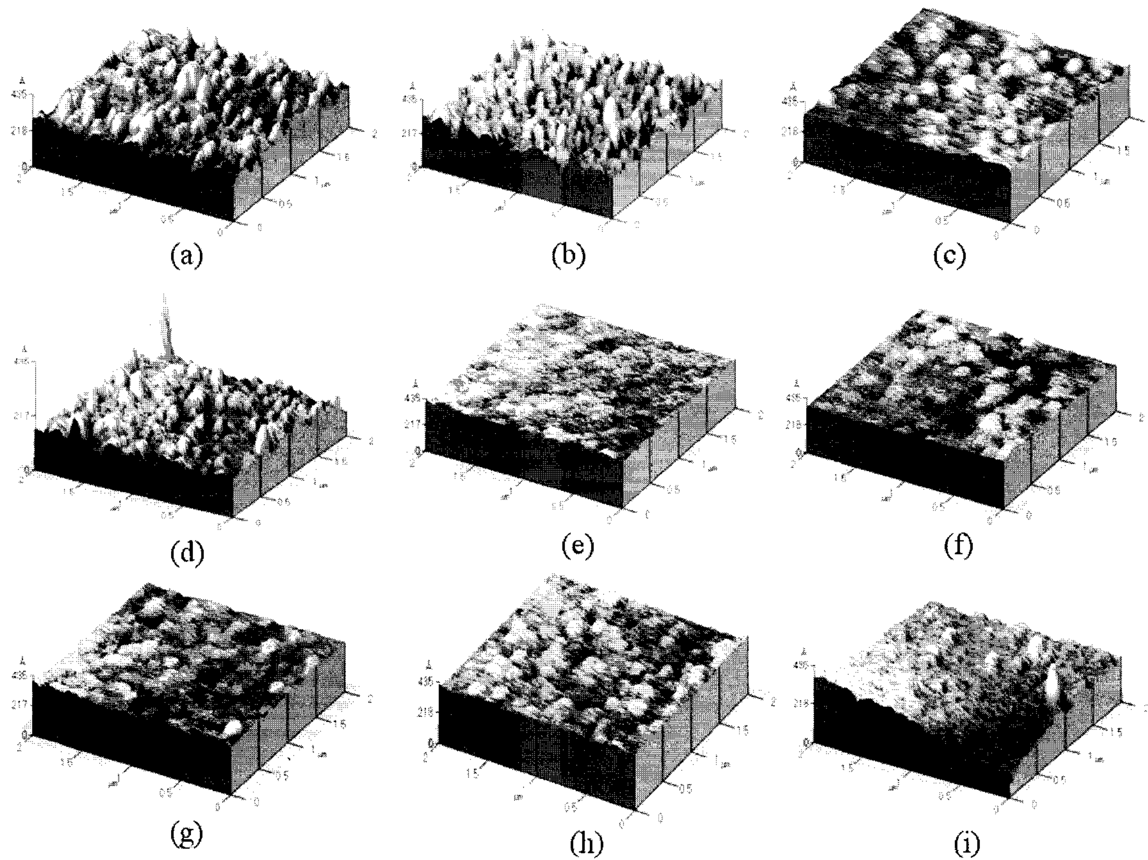

Fig. 3. AFM images of HfO_2 thin films : (a) T_{sub}=450, Ar=3 sccm and O_2=3 sccm, (b) T_{sub}=450, Ar=3 sccm and O_2=5 sccm, (c) T_{sub}=450, Ar=5 sccm and O_2=3 sccm, (d) T_{sub}=450, Ar=5 sccm and O_2=5 sccm, (e) T_{sub}=550, Ar=3 sccm and O_2=3 sccm, (f) T_{sub}=550, Ar=3 sccm and O_2=5 sccm, (g) T_{sub}=550, Ar=5 sccm and O_2=3 sccm, (h) T_{sub}=550, Ar=5 sccm and O_2=5 sccm and (i) T_{sub}=500, Ar=4 sccm and O_2=4 sccm.

The diagnostics of the regression model were represented in Fig. 5. The normal probability for the studentized residuals shows that the straight line is approximately plotted in Fig. 5(a). The studentized residuals show that there are also no patterns and special features in Fig. 5(b). Those values lie in the range between 3 and -3. It could be satisfied with the normality assumption and properties for the residuals[13,14]. In Fig. 5(c), the outlier T plot shows that the some of outlier T values are out of the standard deviation limits between 3.5 and -3.5. It means that there are a few noises in the regression model.

The main effect plots were illustrated in Fig. 6. Of the three main factors, the substrate temperature is potentially impact on the regression model. The other factors, Ar and O_2 flow rate, are effective a little. The interaction plots were illustrated in Fig. 7. The interactions of Ar and O_2 flow rate with the substrate temperature for the response are statistically significant, respectively. The interaction factor is more significant when Ar flow rate with the substrate temperature is the lower than the higher. In contrast, the interaction factor is more significant when O_2 flow rate with the substrate temperature is the higher.

The regression model and the surface plots were illustrated in Fig. 8. The result is summarized in the experimental data versus predicted data as shown in Fig. 8(a). The spots along the straight line in the result mean that the regression model is a good agreement well. As shown in Fig. 8(b) and (c), the contour plot and 3-D surface plot indicate that the overall responses for the various conditions when O_2 flow rate is fixed as 4 sccm.

The half normal and normal probability plots for the factors in the variable transformation model were represented in Fig. 9. Considering the factor effects, the large effect factors in the model using the variable transformation model are two main factors and one interaction factor. The main factors are the substrate temperature and Ar flow rate, and the interaction effect is the factor between the substrate temperature and Ar flow rate.

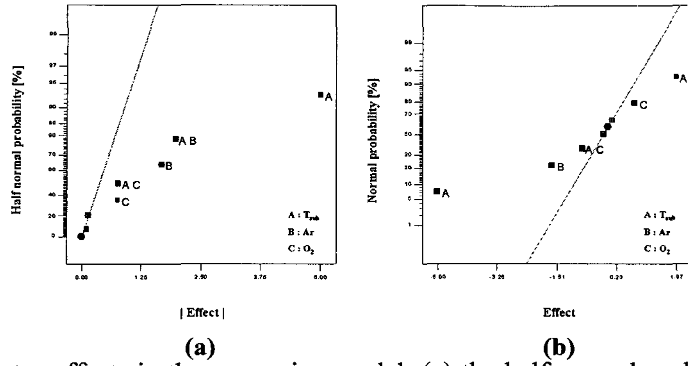

Fig. 4. The plots for the factor effects in the regression model: (a) the half normal probability plot and (b) the normal probability plot.

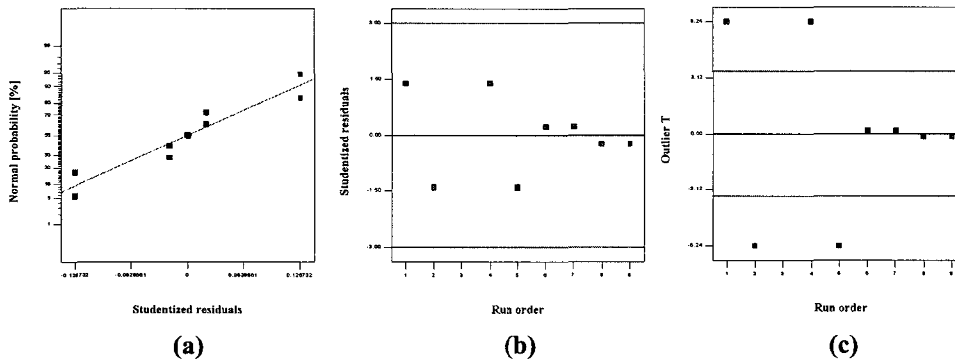

Fig. 5. The plots for the model diagnosis: (a) the normal probability plot for studentized residuals, (b) the studentized residual plot and (c) the outlier T plot.

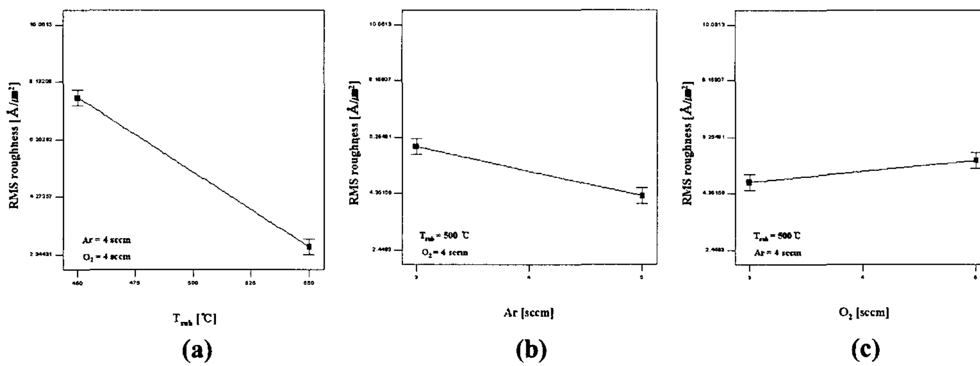

Fig. 6. The main effect plots in the regression model for the RMS roughness: (a) T_{sub}, (b) Ar and (c) O_2.

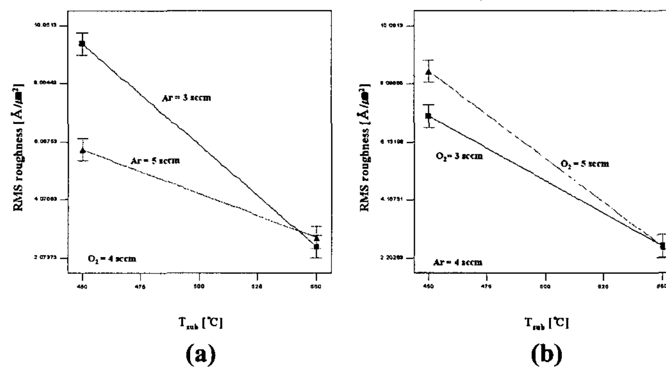

Fig. 7. The interaction effect plots in the regression model for the RMS roughness: (a) O_2=4 sccm and (b) Ar=4 sccm.

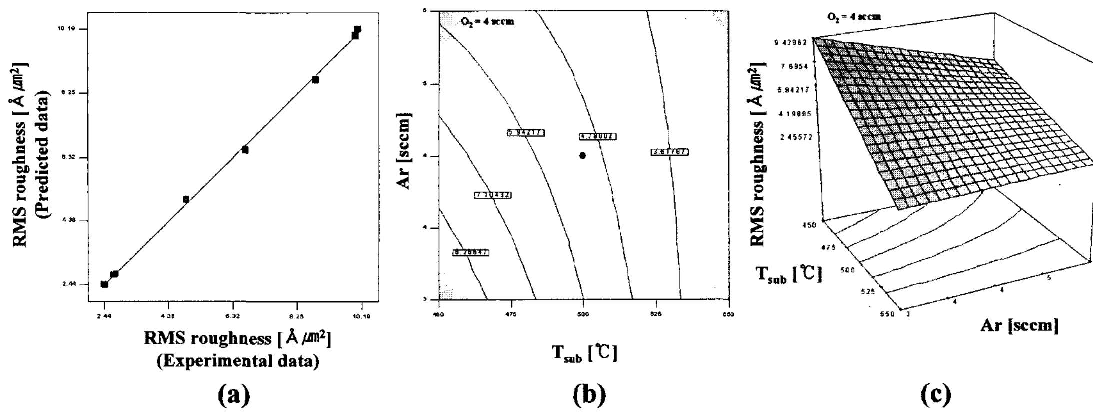

Fig. 8. The regression model results for the RMS roughness: (a) the experimental data vs. the predicted data, (b) the contour plot and (c) the 3-D surface contour plot.

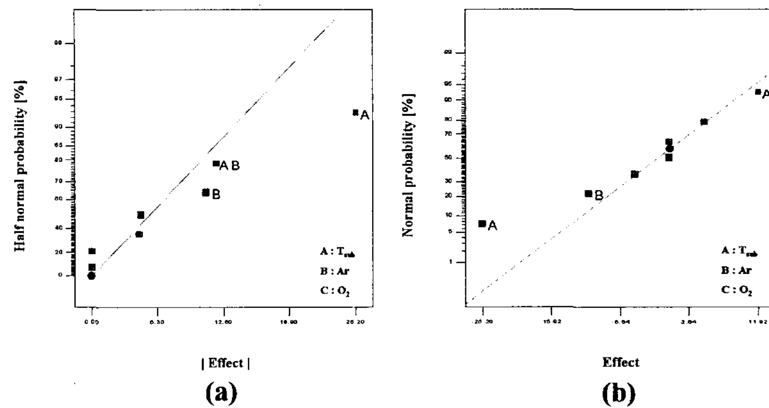

Fig. 9. The plots for the factor effects in the variable transformation model: (a) the half normal probability plot and (b) the normal probability plot.

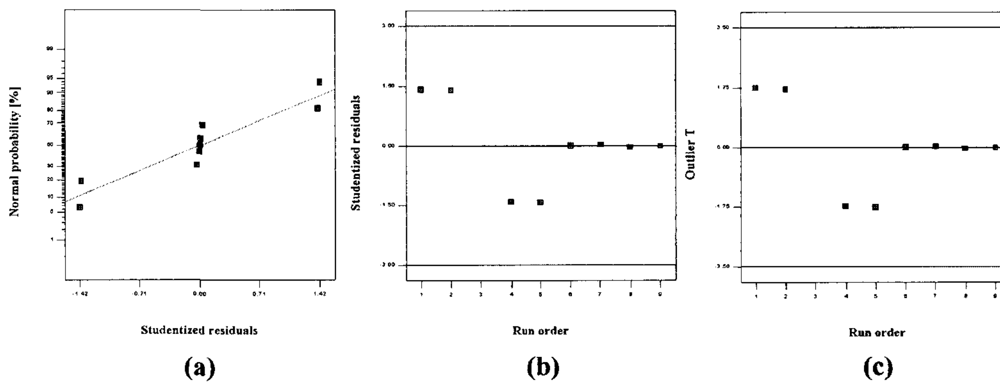

Fig. 10. The plots for the variable transformation model diagnosis: (a) the normal probability plot for studentized residuals, (b) the studentized residual plot and (c) the outlier T plot.

The diagnostics for the variable transformation model were represented in Fig. 10. The normal probability and residual plots for the studentized residuals in Fig. 10 (a) and (b) show that those plots are considerably equal to that of the regression model. On the other hands, unlikely the outlier T plot for the general regression model, there are no values out of the range of between 3.5 and -3.5 in the variable transformation model.

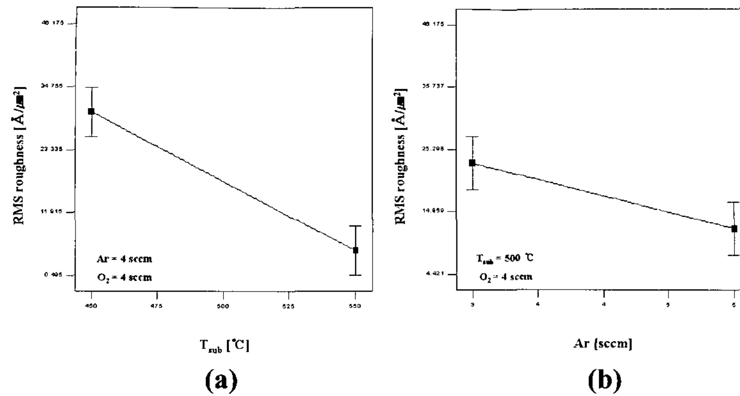

Fig. 11. The main effect plots in the variable transformation model for the RMS roughness: (a) T_{sub} and (b) Ar.

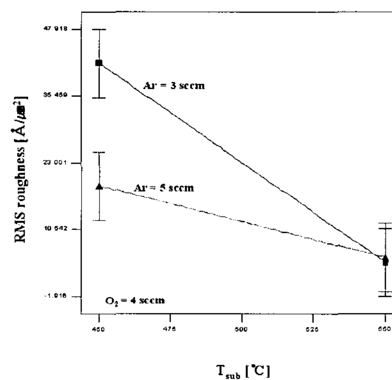

Fig. 12. The interaction effect plots in the variable transformation model for the RMS roughness: T_{sub}.

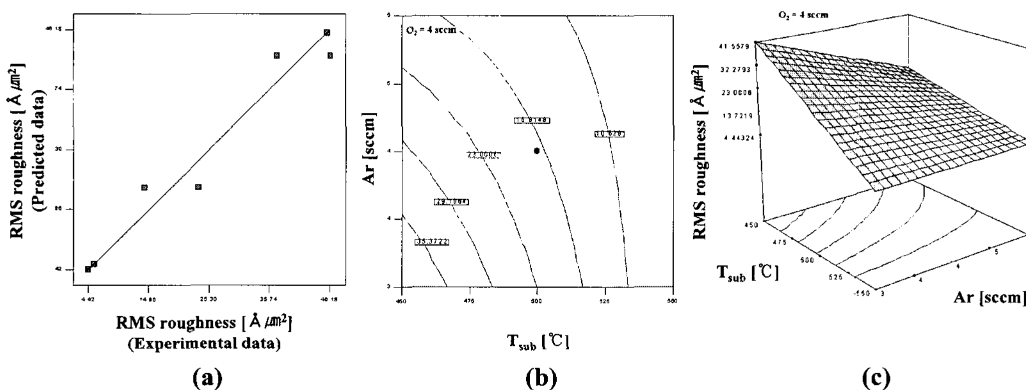

Fig. 13. The variable transformation model results for the RMS roughness: (a) the experimental data vs. the predicted data, (b) the contour plot and (c) the 3-D surface contour plot.

The main effect plots were illustrated in Fig. 11. The substrate temperature effect is higher than the Ar flow rate. The interaction plots were illustrated in Fig. 12. The interaction between the substrate temperature and Ar flow rate is only effective in this model. The interaction factor is more significant when Ar flow rate with the substrate temperature is the lower value.

The regression model and the surface plots were illustrated in Fig. 13. The result was summarized in the experimental data versus predicted data as shown in Fig. 13(a). Even though the accuracy of the variable transformation model is lower than the regression model, the adjusted R-squared values for all models are over 90 %. Nevertheless, that model can be enough to explain the overall response by the reduced variables and the transformed response.

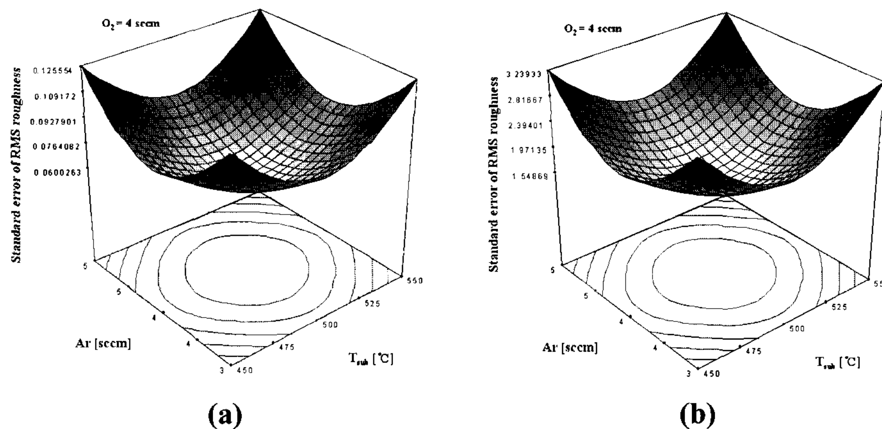

Fig. 14. The 3-D surface plots for the standard error of the RMS roughness: (a) the regression model and (b) the variable transformation model.

The standard error of the RMS roughness for the general regression and the variable transformation model were shown in Fig. 14, these plots exhibit that the variability of the standard error for the response with the process conditions when O_2 flow rate is fixed as 4 sccm.

5. CONCLUSION

The effect analysis for the surface roughness of HfO_2 thin films has been investigated. The general regression model and the variable transformation model were used to build the model to be predicted and analyzed the factor effect and response. As the results, comparing the general regression model with the variable transformation model, the comprehensive model trends can be simply explained by the variable transformation model having the sufficient adjusted R-squared value. The variable transformation model is more effective for analyzing the parameter effect of the model and it could be useful for finding the improved model in the semiconductor manufacturing process.

ACKNOWLEDGMENTS

This research was supported by the MIC(Ministry of Information and Communication), Korea, under the ITRC(Information Technology Research Center) support program supervised by the IITA(Institute of Information Technology Advancement) (IITA-2006-(C1090-0603-0012).

REFERENCES

[1] D. K. Sarker, E. Desbiens, and M. A. El Khakani, “High-k titanium silicate dielectric thin films grown by pulsed-laser deposition”, Appl. Phys. Lett., Vol. 80, No. 2, p. 294, 2002.

[2] D. Brassard, D. K. Sarkar, and M. A. Khakani, “High-k titanium silicate thin films grown by reactive magnetron sputtering for complementary metal oxide semiconductor applications”, J. Vac. Sci. Technol., Vol. A22, No. 3, p. 851, 2004.

[3] D. Brassard, D. K. Sarkar, and M. A. Khankani, “Tuning the electrical resistivity of pulse laser deposition TiSiOx thin films from highly insulating to conductive behaviors”, Appl. Phys. Lett., Vol. 84, No. 13, p. 2304, 2004.

[4] G. Scarel, S. Spiga, C. Wiemer, G. Tallarida, S. Ferrari, and M. Fanciulli, “Trends of structural and electrical properties in atomic layer deposited HfO_2 films”, Mater. Sci. Eng., Vol. 109, No. 1-3, p. 11, 2004.

[5] J. Aarik, H. Mander, M. Kirm, and L. pung, “Optical characterization of HfO_2 thin films grown by atomic layer deposition”, Thin Solid Films, Vol. 466, No. 1-2, p. 41, 2004.

[6] K.-Y. Cha, T.-Y. Tou, and B.-S. Teo, “Effects of substrate temperature on electrical and structural of copper thin films”, Microelectron. J., Vol. 37, p. 930, 2006.

[7] K.-Y. Cha, T.-Y. Tou, and B.-S. Teo, “Thickness dependence of the structural and electrical properties of copper films deposited by dc magnetron sputtering technique”, Microelectron. J., Vol. 37, p. 608, 2006.

[8] S. Samukawa and S. J. Hong, “Statistical characterization fabricated charge-up damage sensor”, Trans. EEM, Vol. 6, No. 3, p. 87, 2005.

[9] Gary S. May, S.-S. Han, and S. J. Hong, “Characterization of low-temperature SU-8 negative photoresist processing for MEMS applications”, Trans. EEM, Vol. 6, No. 4, p. 135, 2005.

[10] K. K. Low and Stephen W. Director, “An efficient

methodology for building macromodels of IC fabrication processes", IEEE Trans. Computer-Aided Design, Vol. 8, No. 212, p. 1299, 1989.
[11] K. Park and J.-H. Ahn, "Design of experiment considering two-way interactions and its application to injection molding processes with numerical analysis", J. Mater. Process. Tech., Vol. 146, p. 221, 2004.
[12] M. Hajeeh, "Estimating corrosion: a statistical approach", Mater. Desi., Vol. 24, p. 509, 2003.
[13] D. C. Montgomery, "Design and Analysis of Experiments", New York: John Wiley & Sons, 1997.
[14] R. H. Myers and D. C. Montgomery, "Response Surface Methodology", New York: John Wiley & Sons, 1995.